IEEE Access
Multidisciplinary | Rapid Review | Open Access Journal

Received November 25, 2021, accepted December 11, 2021, date of publication December 14, 2021,
date of current version December 27, 2021.

Digital Object Identifier 10.1109/ACCESS.2021.3135536

Improved Feature Selection Method for the Identification of Soil Images Using Oscillating Spider Monkey Optimization

RAHUL AGARWAL[1], NARPAT SINGH SHEKHAWAT[1], SANDEEP KUMAR[2], (Member, IEEE), ANAND NAYYAR[3,4], (Senior Member, IEEE), AND BASIT QURESHI[5], (Member, IEEE)

[1]Department of Computer Science and Engineering, Engineering College Bikaner, Bikaner 334004, India
[2]Department of Computer Science and Engineering, CHRIST (Deemed to be University), Bengaluru, Karnataka 560074, India
[3]Graduate School, Duy Tan University, Da Nang 550000, Vietnam
[4]Faculty of Information Technology, Duy Tan University, Da Nang 550000, Vietnam
[5]Department of Computer Science, Prince Sultan University, Riyadh 11586, Saudi Arabia

Corresponding authors: Sandeep Kumar (sandpoonia@gmail.com) and Anand Nayyar (anandnayyar@duytan.edu.vn)

This work was supported in part by the Robotics and Internet of Things Laboratory, Prince Sultan University, Riyadh, Saudi Arabia.

ABSTRACT Precision agriculture is the process that uses information and communication technology for farming and cultivation to improve overall productivity, efficient utilization of resources. Soil prediction is one of the primary phases in precision agriculture, resulting in good quality crops. In general, farmers perform the soil prediction manually. However, the efficiency of soil prediction may be enhanced by using current digital technologies. One effective way to automate soil prediction is image processing techniques in which soil images may be analyzed to determine the soil. This paper presents an efficient image analysis technique to predict the soil. For the same, a robust feature selection technique has been incorporated in the image analysis of soil images. The developed feature selection technique uses a new oscillating spider monkey optimization algorithm (OSMO) for the selection of features that are relevant and non-redundant. The new oscillating spider monkey optimization algorithm increases precision and convergence behavior by using an oscillating perturbation rate. A set of standard benchmark functions was deployed to visualize the performance of the new optimization technique (OSMO), and results were compared based on mean and standard deviation. Furthermore, the soil prediction approach is validated on a soil dataset, having seven categories. The proposed feature selection method selects the 41% relevant features, which provide the highest accuracy of 82.25% with 2.85% increase.

INDEX TERMS Soil prediction, feature selection, spider monkey optimization, perturbation rate, smart agriculture.

I. INTRODUCTION

Worldwide, agriculture is one of the significant sources of food and income. The economy of various countries highly depends on the outcome of agriculture. Different types of plants are harvested according to geographical locations and soil quality. There is a direct relationship between the soil, and the plants [1]. For each plant, a specific soil is required. Soil texture affects agriculture, selection of crops, the requirement of nutrients and water, and growth of crops. Therefore, it is essential to predict the soil before farming.

Furthermore, the selection of plants according to the soil will increase productivity. In general, the soil is predicted manually by farmers as the availability of experts is not easy at all times. This manual process further may be biased and non-appropriate due to the expertise and knowledge of the farmers [2]. Therefore, the automation of soil prediction with precision may improve this selection and may be helpful to increase productivity without the need for an expert. Furthermore, precision agriculture tries to bring farmers and soil closer and work in synchronization. It uses technology and intelligent devices that are interactive and easy to use in farming.

In general, the soil may be classified according to its texture into seven classes; namely, silty sand, clay, sandy clay,

The associate editor coordinating the review of this manuscript and approving it for publication was Alberto Cano.

clayey sand, clayey peat, humus clay, and peat [3], [4]. The pipette and hydrometer methods are the primary method of predicting the soil, which is time-consuming and requires an extensive workforce. Moreover, the most common soil analysis approach to study soil sub-surface with soil surface depth information is known as cone penetration testing (CPT) [5], [6]. However, Zhang *et al.* [7] observed that this CPT method may give uncertain results due to the complex composition and varying mechanical properties of soil. It results in class overlapping of different soils.

Furthermore, CPT and hydrometer methods are not easily approachable to each farmer. Recently, digital image processing provides very effective classification techniques that can be utilized to select soil according to its texture. Therefore, in this work, a soil prediction method has been developed using image analysis techniques that use the texture images of soil for its classification.

Past several years witnessed different soil classification methods [3], [8], [9]. Chung *et al.* [10] use RGB histogram techniques to represent the paddy soil series. Sharma and Kumar [11] presented traditional image mid-level and high-level classification methods for the classification of soil. Bhattacharya *et al.* [3] extracted the features using the boundary energy technique after the segmentation of signals. For the classification task, various classifiers are used and validated like neural networks, decision trees, support vector machine (SVM), and many others. Furthermore, Gordon reviewed the SVM classifiers in soil classification using image-based features and observed that the efficiency of these techniques is highly affected by how features are extracted.

Since the classification accuracy is heavily dependent on the quality of extracted features [12], [13], various feature extraction methods for soil classification have been presented. These feature extraction techniques are general statistics and learning-based. The methods of learning-based feature extraction use machine learning for feature extraction from soil images. Some popular machine learning approaches in this category are convolutional neural network (CNN) [14], restricted Boltzmann machines [15], and auto-encoders [16]. Feature selection problem is a combinatorial optimization problem, recently Shi *et al.* [17] proposed a collaborative approach for dimensionality reduction, and Li and Du [18] deployed the Laplacian method for analyzing hyperspectral imagery. Padarian *et al.* [19] used a CNN model to predict the soil organic carbon and showed that it reduces the error by 30%. Lu *et al.* [20] presented a 4 layers deep CNN for soil detection. For the same, they have used the combination of 80 synthetic hyperspectral bands and eight multispectral bands to improve the soil prediction accuracy by 7.42%. Furthermore, Yu *et al.* [21] proposed a three-dimensional CNN for soil classification and accelerated the feature discriminator's ability. Thuy and Wongthanavasu [22], [23] proposed two new approaches for feature selection; the first approach is based on D-stripped quotient sets, and the second is based on stripped neighborhood. In literature, these learning-based feature extraction methods perform well. Swarm-based techniques [24], [25] are successfully deployed for solving different real-world problems. However, a high computational cost is induced in these approaches.

The statistical techniques extract different sizes, shapes, and structural features from the soil images further supplied to one of the classifiers. These methods do not generally perform well due to the complexity of an image's texture. Recently, different texture feature-based methods have been implemented to take out the features of an image like local binary pattern (LBP) [26], the histogram of oriented gradient (HOG) [27], speed-up Robust Features (SURF) [28], and scale-invariant feature transform (SIFT) [29]. These feature extraction methods show better performance for complex structured images. However, these methods generate high-dimensional feature maps that may lead to the generation of irrelevant and redundant features. These redundant and irrelevant features are responsible for the degraded performance of a classification system [30]. Therefore, this work uses a powerful feature selection approach to reduce redundant and irrelevant features.

In literature, many feature selection methods are present, which can be categorized into wrappers, filters, and embedded methods [31]. The filter method is computationally efficient because it uses feature maps as class variables. However, these filter methods do not perform well when used as a classifier [32]. In the case of wrapper methods, predictive models are used to find the feature subset such as Sequential backward selection (SBS) [33] method. These methods are more promising than the filter methods [31] and iteratively remove the irrelevant features. Finally, embedded methods use classifiers to find a good set of features such as SVM with recursive feature elimination (SVM-RFE) [34]. The primary concern with the wrapper and embedded methods are their computational complexity which is very high [12].

Graph-based techniques are also successfully deployed for feature selection. Roffo *et al.* [35] proposed a framework for feature selection using Markov chain and power series of matrices. Hashemi *et al.* [36] introduced a multi-label graph-based approach. Here, the author used the PageRank algorithm. Henni *et al.* [37] deployed PageRank algorithm with subspace for feature selection using a graph-based unsupervised algorithm. Roffo *et al.* [38] introduced a graph-based ranking system with probabilistic latent. Zhang and Hancock [39] introduced hypergraph clustering in feature selection. Chen *et al.* [40] used these algorithms for object-oriented classification.

Classical search strategies are single solution-based techniques for optimization, and the result is also one optimized solution. These classical optimization methods cannot solve problems that are non-differentiable, discrete, and multi-model. Thus, it is required to use some approaches to handle these complexities. Population-based approaches are one of the best solutions and emerging techniques. These algorithms use a swarm of solutions in every cycle and result in a population of solutions. Population-based algorithms share numerous mutual conceptions. Due to the capability of handling a

large class of problems, this research work considered SMO as the center of research. The use of meta-heuristic methods generally removes the drawbacks of the feature, as mentioned earlier, selection methods. Different researchers presented various meta-heuristic algorithms to efficiently select features from high-dimensional feature maps. For example, the spider monkey optimization (SMO) [41] algorithm is a nature-inspired algorithm based on the behavior of spider monkeys. SMO has been proved better for handling high-dimensional feature space, which may be helpful in feature selection. The algorithm looks over the search area in its initial phases and then exploits it iteratively. For the same, the SMO uses the social organization of spider monkeys. SMO has been used in various real-world optimization problems successfully. Hybrid of SMO with other NIA [42] also deployed for information retrieval and performed well. However, its performance may be improved by modifying its different parameters.

In SMO, different phases are used, like the global and local leader phases, which are highly affected by a parameter known as perturbation rate. It is an essential parameter of SMO for deciding its convergence behavior. In standard SMO, a linearly increasing perturbation rate is used. Although this linear increasing function performs well but not so well for non-linear real-world problems, the inclusion of non-linearity in perturbation rate may increase the performance of new variants. Considering the same, different researchers have used different non-linear perturbation rates. For example, Kumar *et al.* [43] used a chaotic SMO in bag-of-words for soil prediction in which chaotic perturbation is used.

Moreover, an exponential perturbation rate is used in SMO for plant leaf disease identification [44]. However, these variations also converge towards the local optima. Hence, improvement in the perturbation rate is still an open area. Therefore, this paper introduces a new approach (OSMO) in which the perturbation rate oscillates between a range and improves the balancing of exploitation and exploration. Furthermore, the proposed OSMO has been used to select the optimum set of features from high dimensional feature vectors of soil images.

The major research contributions of this paper are as follows:

1) A detailed study was conducted for recent modifications in SMO and recent development in plant disease identification.
2) A new oscillating perturbation rate was introduced in SMO and named the oscillating SMO (OSMO) algorithm.
3) The texture features are obtained from the images using the SURF method, and OSMO-based feature selection enhances the classification accuracy.
4) The performance of OSMO was evaluated on 15 benchmark problems, and results were validated by Wilcoxon rank-sum test.
5) Soil images are classified by SVM, LDA, kNN, and RF classifiers. These algorithms are compared for the number of features selected and the accuracy achieved.
6) The RF classifier achieved the best accuracy (82.25%) for the OSMO-based feature selection approach with a 2.85% increase.

The rest of the paper is as follows. The standard SMO is briefed in Section II followed by the OSMO algorithm in Section III. Section IV contains result discussion and statistical validation of achieved results. Section V concludes the paper with future scope.

II. SPIDER MONKEY OPTIMIZATION (SMO)

The SMO algorithm is driven by spider monkeys' social and foraging behavior. The fission-fusion social structure (FFSS) is used to model the SMO algorithm, in which monkeys divide themselves into groups from large to small and vice-versa. The following are the essential characteristics of FFSS in spider monkeys [41].

1) All the spider monkeys maintain a group of 40 to 50 monkeys known as individuals in SMO.
2) There is a global leader (GL) among the monkeys who can divide the groups into smaller three to eight subgroups if the food is insufficient. Each group starts foraging independently.
3) Each subgroup also has a local leader (LL) under which the food is searched.
4) The group members use a unique sound to social interaction with other members of the group's

As mentioned earlier, the basis of foraging among spider monkeys, the SMO, has been mathematically designed and developed. In SMO, there are six phases and discussed in subsequent subsections. The Algorithm 1 illustrates the pseudo-code for the standard SMO.

Let i^{th} individual (X_i) in a D-dimensional vector of N population is represented by Eq. (1) and initialized by Eq. (2).

$$X_i = X_i^1, X_i^2, \ldots, X_i^j, \ldots X_i^D \tag{1}$$

$$X_i^j = X_{min}^j + \phi \times (X_{max}^j - X_{min}^j) \tag{2}$$

where X_{max}^j and X_{min}^j are upper and lower value of X_i in the j^{th} dimension. ϕ returns an arbitrary number in the range of [0, 1].

A. LOCAL LEADER PHASE (LLP)

This phase updates the location (X_i^j) of each member using the learning of the LL (XL_k^j) and members of the local group by Eq. (3), based on a probability pr that is known as perturbation rate. This position is only updated if a new solution has higher fitness than the existing solution.

$$X_i^j = X_i^j + \phi \times (XL_k^j - X_i^j) + \psi \times (X_r^j - X_i^j) \tag{3}$$

here, $\psi \in [-1, 1]$ is a random number, XL_k^j is the positions of the LL in k^{th} group and X_r^j is randomly selected r^{th} individual from this group.

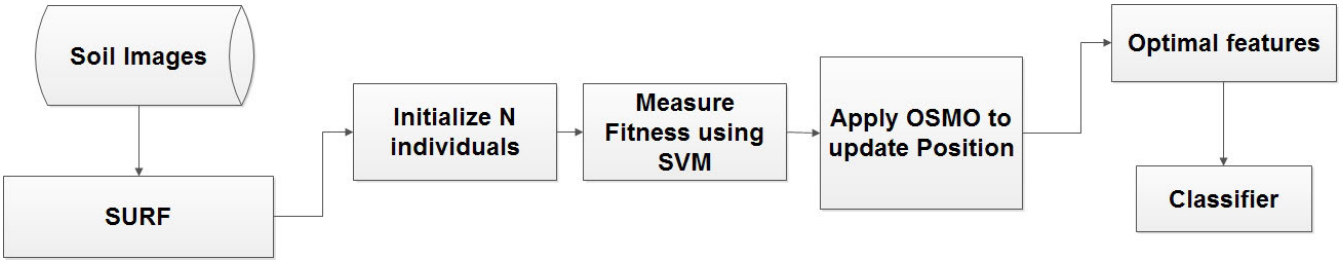

FIGURE 1. The proposed OSMO based soil image classification method.

Algorithm 1 Spider Monkey Optimization

Randomly initialize the swarm of N monkeys. That denote a vector of D decision variables, depicted as $\{X_i^1, X_i^2, \ldots, X_i^j, \ldots X_i^D\}$. Here, i is the i^{th} individual.
Randomly initializes pr and limit for Local and Global Leader.
Measure, the fitness of each individual.
Elect local and global leaders using greedy selection process.
while Stopping Criteria **do**
  Obtain new positions for all individuals using the Local leader phase.
  Use the fitness values of each group member to deploy the greedy selection.
  Apply the global leader phase to obtain the group members' new positions.
  The location of global and local leaders is updated based on fitness.
  If there is no change in any Local group leader for a predefined limit, apply the LLD phase.
  If Global Leader is not updated for a predefined limit, then apply the GLD phase to divide the group into smaller subgroups. Maintain the minimum size of each group to four.
end while

B. GLOBAL LEADER PHASE (GLP)

After the LLP, every individual updates its location using Eq. (4). This phase includes the knowledge of GL (XG_j) and members of the local group.

$$X_i^j = X_i^j + \phi \times (XG_j - X_i^j) + \psi \times (X_r^j - X_i^j) \quad (4)$$

C. GLOBAL LEADER LEARNING (GLL) PHASE

In the GLL phase, the best individual is declared as a global leader (XG_j). If the GL fails to update her position, it increments the global limit counter.

D. LOCAL LEADER LEARNING (LLL) PHASE

The monkey (Solution) with the highest fitness is elevated as LL (XL_k^j) of a particular group during the LLL phase. Similar to the previous step, if the position of LL does not change, then the counter for the local limit is incremented by one.

E. LOCAL LEADER DECISION (LLD) PHASE

This phase either randomly initializes all the group members or modifies their position using Eq. (5) based on the counter for local limit.

$$X_i^j = X_i^j + \phi \times (XG_j - X_i^j) + \psi \times (X_r^j - X_i^j) \quad (5)$$

F. GLOBAL LEADER DECISION (GLD) PHASE

If the count of global limit for a GL (XG_j) outstretched a threshold, then the GL creates smaller subgroups until the maximum number of groups (MG) is achieved. This phase also selects the LL's (XL_k^j) by using the LLL phase. On the other hand, if the location of GL remains the same until the threshold MG, then it fuses all the small groups into a large group.

III. OSMO BASED SOIL IMAGE CLASSIFICATION

The proposed approach presents a new soil prediction method using the soil images. First, the method identifies the category of soil in three simple steps as given in Fig. 1. The 1^{st} step is the extraction of features from the considered soil images followed by the second step selection of features. The primary research outcome of this work is the development of the second step, i.e., feature selection. A new approach (OSMO) has been introduced in feature selection to select optimum features. The identified prominent features are then made available to the classification phase, where a classifier is trained to recognize the soil quality. Each phase of the proposed methodology is described in the upcoming subsections.

A. FEATURE EXTRACTION

The first step of the proposed soil classification system is extraction features. For the same, texture features are extracted from the images using the SURF technique. The SURF technique for feature extraction was developed by Bay *et al.* [28] which extracts the local features and corresponding descriptor. Generally, SURF is used to extract the texture features in various application areas of computer vision. The features extracted by SURF are rotational, illumination, scale, and noise invariant. This technique works in three phases: detecting interest points, neighborhood description, and keypoint matching. First, the Hessian matrix approximation finds the interest points in the image. Then, the sum of Haar wavelet responses among the neighborhood is

measured for the feature descriptor. Finally, keypoint matching is performed between the descriptors.

B. OSCILLATING SMO BASED FEATURE SELECTION

After the SURF features extraction method, a high-dimensional feature map is generated. Due to its high dimension, the computation cost of a classification system increases. Furthermore, some of these features may be redundant and irrelevant, reducing the efficiency of a deployed classifier. Therefore, to minimize these two effects, a new feature selection approach has been presented in this paper. The newly presented feature selection approach uses an OSMO algorithm to select the optimum features. OSMO is an optimization algorithm that finds the optimum solution in a guided search and variant of the existing SMO algorithm. The steps of the proposed feature selection method are as follows.

1) Let D features are extracted by the SURF method. These features are represented in a one-dimensional vector.
2) Initialize the N individuals in the population of the OSMO algorithm randomly in the range of [0, 1]. The dimension of every solution is equated to the count of features, ie. D and is represented by $\{X_i^1, X_i^2, \ldots, X_i^j, \ldots X_i^D\}$ as depicted in Eq. 1.
3) Initialize limit for Global and Local Leader and pr randomly.
4) Calculate the fitness of every solution as follows:
   a) Convert the decision variables values of each individual from real to binary using a threshold value (Th) and Eq. (6). The value of (Th) can be selected empirically.

$$X_i^j = \begin{cases} 1 & if \;\; X_i^j > Th \\ 0 & if \;\; X_i^j \leq Th \end{cases} \tag{6}$$

   b) Use the accuracy returned by K-fold cross SVM as the fitness value of an individual. The input to the SVM classifier is those features whose X_i^j value is 1 and the corresponding image label.
5) Apply the OSMO algorithm to find the best individual.
6) Select those features whose corresponding X_i^j value is 1 in the best individual returned by the OSMO algorithm.

The proposed OSMO algorithm is similar to the SMO algorithm except for the perturbation rate. In basic SMO, the perturbation rate increases linearly, while an oscillating perturbation rate is introduced in the newly proposed OSMO algorithm and is explained in the following subsection.

1) OSCILLATING PERTURBATION RATE

The perturbation rate, an essential parameter of SMO, dramatically impacts the precision and rate of convergence. The basic SMO has a linearly increasing perturbation rate. However, as the maximum problems in the real world are nonlinear, non-linearity in the perturbation rate can improve SMO's performance. Recently Kumar *et al.* [43], [44] proposed chaotic SMO [43] and exponential SMO [44] for soil classification and leaf image classification respectively. These two modifications in SMO taken advantage of the nonlinear perturbation rate. The chaotic map used by [43] to decide perturbation rate is illustrated by Eq. (7).

$$pr_{(t+1)} = 1 - (pr_t) \times \left(\frac{max\_it - t}{max\_it}\right) \times z \tag{7}$$

where, t and max_it represent current iteration and maximum number of iterations respectively. The value of z is decided by Eq. (8)

$$z_{(t+1)} = \mu \times z_t \times (1 - z_t) \tag{8}$$

where, $z_t \in [0, 1]$ represent chaotic number for t^{th} generation. Value of μ is fixed 4 for this experiment after exhaustive experiments.

In exponential SMO [44], the perturbation rate, is increased exponentially with the help of exponential function as illustrated in Eq. (9)

$$pr_{new} = (pr_{init})^{\frac{max\_it}{t}} \tag{9}$$

where, t and max_it represent current iteration and maximum number of iterations respectively and pr_{init} in initial rate of perturbation that is randomly initialized in the range of 0 and 1.

Keeping these modifications in mind, this paper proposes a new oscillating perturbation rate which is inspired by the oscillating inertia weight in PSO [48]. In OSMO, the rate of perturbation is updated as per its oscillating behavior, which can be implemented by the following Eq. (10).

$$pr(t) = \frac{Pr_{min} + Pr_{max}}{2} + \frac{Pr_{max} - Pr_{min}}{2} cos(\frac{2\pi t}{T}) \tag{10}$$

$$T = \frac{2S_1}{3 + 2k} \tag{11}$$

where, Pr_{min} and Pr_{max} are the oscillating range of Pr. The value of t represents the t^{th} iteration. T is the oscillation period, and k is a constant integer value in the range of [1, 7]. S_1 is the count of iterations for which Pr oscillates, and for the remaining iterations, its value is kept constant. This way, the Pr oscillates for S_1 number of iterations and remains the same as other iterations.

C. SOIL IMAGE CLASSIFICATION

In the final step of soil image classification, a classifier is used that is trained using selected features and the corresponding image labels. The proposed OSMO algorithm selects the features. This paper uses four classifiers for classification: k-nearest neighbors, Linear discriminant analysis (LDA), SVM, and random forest (RF). The SVM classifies the data with the help of a defined hyper-plane. This paper uses a multi-class SVM classifier for the classification of soil images. LDA uses a linear combination of features to discriminate against the classes. K-nearest neighbors classifier stores all available cases and categorizes new objects based

TABLE 1. Standard benchmark functions [43], [45]–[47].

Fn. No.	Equation	Optimal Value	Range	Dimensions
Sphere (F_1)	$\sum_{i=1}^{d} x_i^2$	0	[-100,100]	30, 50
Schewel (F_2)	$\prod_{i=1}^{d} \mid x_i \mid + \sum_{i=1}^{d} \mid x_i \mid$	0	[-10,10]	30, 50
Schwefel 2.21 function (F_3)	$max_i\{\mid x_i \mid, 1 \leq i \leq d\}$	0	[-100,100]	30, 50
Step Function (F_4)	$\sum_{i=1}^{d}([0.5 + x_i])^2$	0	[-100,100]	30, 50
Quartic Function (F_5)	$\sum_{i=1}^{d} ix_i^4 + random[0, 1)$	0	[-1.28,1.28]	30, 50
Ackley 1 Function (F_6)	$20 + e - exp\left(\frac{1}{d}\sum_{i=1}^{d} cos(2\pi x_i)\right) - 20exp\left(-0.2\sqrt{\frac{1}{d}\sum_{i=1}^{d} x_i^2}\right)$	0	[-32,32]	30, 50
Levy Montalvo 2 (F_7)	$0.1\{\sum_{i=1}^{d}(x_i-1)^2[1+\sin^2(3\pi x_i+1)]+\sin^2(3\pi x_1)+(x_d-1)^2[1+\sin^2(2\pi x_d)]\}+\sum_{i=1}^{d} u(x_i,5,100,4)$	0	[-50,50]	30, 50
Rosenbrock Function (F_8)	$\sum_{i=1}^{n-1}\left[100(a_{i+1}-a_i^2)^2+(a_i-1)^2\right]$	0	[-30,30]	30, 50
F_9	$\sum_{i=1}^{n}[a_i^2 - 10\cos(2\pi a_i) + 10]$	0	[-5.12,5.12]	30, 50
Levy Montalvo 1 (F_{10})	$\frac{\pi}{n}\left\{\sum_{i=1}^{n-1}(y_i-1)^2\left[1+10\sin^2(\pi y_1)\right]+(y_n-1)^2\right\}+10\sin(\pi y_1)+\sum_{i=1}^{n} u(a_i,10,100,4),\ y_i = 1+\frac{a_i+1}{4},$ $u(a_i,x,k,m) = \begin{cases} k(a_i-x)^m & a_i > 0 \\ 0 & -x < a_i < 1 \\ k(-a_i-x)^m & -a_i - x \end{cases}$	0	[-50,50]	30, 50
Alpine 1 Function (F_{11})	$\sum_{i=1}^{d} \lvert 0.1x_i + x_i\sin(x_i)\rvert$	0	[-10, 10]	30, 50
Brown Function (F_{12})	$\sum_{i=1}^{d-1}(x_i^2)^{(x_{i+1}^2+1)} + (x_{i+1}^2)^{(x_i^2+1)}$	0	[-1, 4]	30, 50
Griewank Function (F_{13})	$1 + \sum_{i=1}^{d}\frac{x_i^2}{4000} - \prod_{i=1}^{d}\cos(\frac{x_i}{\sqrt{i}})$	0	[-600, 600]	30, 50
Griewank function (F_{14})	$\frac{1}{4000}\sum_{i=1}^{n} a_i^2 - \prod_{i=1}^{n}\cos(\frac{a_i}{\sqrt{i}}) + 1$	0	[-600,600]	30, 50
Schwefel 2.26 function (F_{15})	$\sum_{i=1}^{n} -a_i \sin\sqrt{\lvert a_i\rvert}$	0	[-500,500]	30, 50

TABLE 2. Parameter settings for the proposed OSMO algorithm.

Parameter	Value
Size of Population	50
No. of Iterations	1000
Initial Pr. Value	0.1
k	2
S_1	600

on a similarity measure. RA is an ensemble learning method for classification in which decision trees are used to predict the classes.

IV. EXPERIMENTAL RESULTS

The performance of the oscillating SMO-based feature selection algorithm for the prediction of soil images has been conducted in two phases. The result analysis of the new OSMO algorithm is depicted in phase one, followed by the effectiveness analysis of oscillating SMO-based feature selection method on soil image dataset. The results of both phases are illustrated in the subsequent subsections.

A. RESULTS OF OSCILLATING SMO

For the analysis of the OSMO performance, 15 representative benchmark functions are used. These functions are taken

TABLE 3. Performance analysis (in terms of mean fitness values for 30 and 50 dimensions) of OSMO and other considered algorithms.

Function	Dimension	CSMO	ESMO	IGSA	WOA	PSO	OSMO
F_1	30	3.12E-29	1.63E-28	1.12E-29	1.77E-20	4.11E-21	**1.21E-29**
	50	2.32E-21	1.22E-19	1.70E-21	1.14E-15	2.31E-18	**1.11E-22**
F_2	30	2.66E-21	5.55E-14	1.34E-22	2.11E-12	6.71E-11	**1.38E-21**
	50	3.23E-16	3.41E-10	1.22E-18	1.32E-7	4.22E-7	**1.24E-19**
F_3	30	3.11E-12	2.31E-06	2.33E-14	6.3221	2.11E-07	**6.35E-14**
	50	2.36E-6	1.27E-01	1.21E-07	9.4321	1.31E-01	**2.33E-08**
F_4	30	0.5232	0.8924	1.31E-02	0.9896	0.5792	**4.11E-03**
	50	0.9134	1.2122	1.22E-01	1.2231	0.7129	**1.13E-01**
F_5	30	3.22E-05	1.23E-04	3.32E-06	1.21E-02	3.15E-02	**2.16E-08**
	50	2.21E-01	1.11E-01	2.21E-01	1.11E-00	2.12E-00	**1.11E-02**
F_6	30	2.34E-09	2.46E-09	**2.11E-11**	3.71E-07	2.21E-07	4.32E-11
	50	1.13E-02	1.21E-2	**1.32E-03**	1.22E-02	2.39E-03	1.47E-03
F_7	30	3.12E-06	1.11E-02	2.32E-07	4.96E-01	4.63E-02	**1.33E-09**
	50	1.36E-02	1.42E-00	1.12E-02	2.33E-00	1.34E-00	**1.51E-03**
F_8	30	2.21E-07	2.63E-05	1.61E-03	3.27E-05	2.23E-06	**3.29E-04**
	50	2.39E-02	1.11E-01	1.22E-00	2.24E-01	1.37E-02	**2.34E-03**
F_9	30	1.11E-08	1.92E-06	1.22E-04	1.11E-06	1.22E-07	**1.19E-09**
	50	2.33E-03	1.24E-02	1.31E-01	2.22E-02	1.92E-03	**1.14E-04**
F_{10}	30	**1.11E-10**	2.31E-08	1.52E-06	2.16E-08	2.62E-09	1.42E-07
	50	**1.39E-06**	1.24E-03	1.56E-02	1.14E-03	1.77E-04	1.23E-05
F_{11}	30	2.22E-07	2.31E-08	1.11E-07	3.37E-07	2.81E-06	**1.01E-08**
	50	1.97E-04	1.31E-03	1.74E-01	2.14E-01	1.22E-03	**1.32E-04**
F_{12}	30	3.21E-06	2.22E-04	1.75E-02	1.33E-04	2.54E-05	**2.41E-06**
	50	1.39E-01	1.25E-01	1.72E-01	2.41E-01	1.71E-01	**1.45E-02**
F_{13}	30	1.21E-05	3.32E-03	1.22E-01	1.27E-03	3.24E-04	**1.19E-05**
	50	2.33E-00	1.41E-01	1.43E-01	2.24E-01	1.11E-01	**1.02E-01**
F_{14}	30	**1.34E-09**	2.92E-06	1.75E-05	3.13E-04	2.53E-07	1.29E-08
	50	2.27E-04	1.79E-02	1.13E-02	2.15E-04	1.27E-04	**1.04E-04**
F_{15}	30	2.63E-07	2.24E-05	1.21E-04	3.11E-05	1.23E-06	**2.19E-07**
	50	1.19E-02	1.25E-02	1.12E-01	2.31E-02	1.37E-02	**1.14E-03**

from Kumar *et al.* [43] who have also worked on the soil classification and presented chaotic SMO (CSMO). These functions are depicted in Table 1 [43], [45]–[47] along with the optimum value of each function, range of decision variables, and the considered dimensions. For the comparative analysis, five meta-heuristic algorithms are considered, namely CSMO [43], exponential SMO (ESMO) [44], whale optimization algorithm (WOA) [49], intelligent gravitational search algorithm (IGSA) [50], and PSO [51]. The parameter settings of the proposed OSMO algorithm are given in Table 2. The parameter settings are considered from their literature for all other existing algorithms. However, for all the considered algorithms, the number of iterations and population size is kept to 1000 and 50, respectively. To eliminate the randomization effect, results are averaged for 30 runs, and their mean fitness values are recorded and compared.

The mean fitness values returned by different meta-heuristic algorithms for 30 and 50 dimensions are compared and depicted in Table 3. From the table, it can be seen that the proposed OSMO outperforms the other existing methods for $F_1, F_2, F_3, F_4, F_5, F_7, F_8, F_9, F_{11}, F_{12}, F_{13}, F_{15}$ functions for both the 30 and 50 dimensions. For the F_6 function, IGSA shows the competitive results. In the case of F_{10}, CSMO shows better results. For F_{14}, the proposed OSMO gives better results on 50 dimensions. This validates that the proposed OSMO algorithm converges better than other methods.

Furthermore, the mean fitness value results are statistically validated by using the Wilcoxon rank-sum test [52] for both the dimensions, i.e. 30 & 50 and presented in Tables 4 and 5 respectively. The NULL hypothesis is that with a significance level of 5%, two methods are the same for a benchmark function. In the table, '+' and '=' signify the rejection and acceptance of the NULL hypothesis, respectively. Moreover, '+' specifies that the OSMO algorithm performs better than the corresponding method. From the Wilcoxon rank-sum test table, it is discernible that the OSMO either performs better for the benchmark functions or performs equally than the existing method. The values for F_6, F_{10}, and F_{14} functions with respective to IGSA is '=', which indicate that

TABLE 4. Statistical validation of OSMO algorithm for 30 dimensions using the Wilcoxon rank-sum test for 0.05 significance level.

Function	OSMO-CSMO	OSMO-ESMO	OSMO-IGSA	OSMO-WOA	OSMO-PSO
F_1	+	+	+	+	+
F_2	+	+	+	+	+
F_3	+	+	+	+	+
F_4	+	+	+	+	+
F_5	+	+	+	+	+
F_6	+	+	=	+	+
F_7	+	+	+	+	+
F_8	+	+	+	+	+
F_9	+	+	+	+	+
F_{10}	=	+	+	+	+
F_{11}	+	=	+	+	+
F_{12}	=	+	+	+	+
F_{13}	=	+	+	+	+
F_{14}	=	+	+	+	+
F_{15}	+	+	+	+	+

TABLE 5. Statistical validation of OSMO algorithm for 50 dimensions using the Wilcoxon rank-sum test for 0.05 significance level.

Function	OSMO-CSMO	OSMO-ESMO	OSMO-IGSA	OSMO-WOA	OSMO-PSO
F_1	+	+	+	+	+
F_2	+	+	+	+	+
F_3	+	+	+	+	+
F_4	+	+	=	+	+
F_5	+	+	+	+	+
F_6	+	+	=	+	=
F_7	+	+	+	+	+
F_8	+	+	+	+	+
F_9	+	+	+	+	+
F_{10}	=	+	+	+	+
F_{11}	=	+	+	+	+
F_{12}	+	+	+	+	+
F_{13}	+	=	=	=	=
F_{14}	=	+	+	=	=
F_{15}	+	+	+	+	+

the proposed algorithm gives a similar output as for IGSA and CSMO, respectively. Therefore, these results validate the performance of the OSMO better than the other considered methods.

Figure 3 shows the comparison of features selected by the proposed OSMO algorithm and other considered algorithms, while Figure 4 shows the accuracy comparison for considered algorithms.

B. RESULTS OF OSMO BASED SOIL IDENTIFICATION

A soil image dataset is considered to validate the performance of OSMO based feature selection method. The soil image dataset consists of seven types of images, namely sandy clay, clayey sand, clay, silty sand, peat, clayey peat, and humus clay, [3]. There are 175 images, 25 from each category. A sample image of soil from each class is displayed in Fig. 2. The input images are of different sizes and are RGB-colored images. Hence, the images are reshaped to 250 $\times$ 190. The images are captured from different geographical locations. After extracting features, the efficiency of extracted features is tested on four classifiers, namely RF, LDA, kNN, and SVM.

The performance of the OSMO algorithm-based feature selection mechanism for the soil image dataset is compared with CSMO, ESMO, IGSA, WOA, and PSO-based feature selection approaches. The accuracy of classification and number of selected features are considered as the performance parameters, and the results are illustrated in Table 6. It is discernible from the table that SURF extracted 127054 from the image, and the same is illustrated in Fig 3. Moreover, the table also depicts the number of features selected by the proposed and considered

(a) Clayey sand (b) Silty sand (c) Sandy clay

(d) Humus clay (e) Clay (f) Peat

(g) Clayey peat

FIGURE 2. Sample soil images.

TABLE 6. Comparison of performance for OSMO-based feature selection and classification methods against the existing methods.

Feature Selection Algorithm	No. of Selected Features	% Elimination	SVM	LDA	kNN	RF
None	127054	0	71.38	60.67	62.31	72.42
CSMO	64798	49	77.82	66.33	69.20	78.23
ESMO	59715	53	76.21	65.98	67.65	78.33
IGSA	55903	56	78.39	68.63	71.10	79.97
WOA	67339	47	74.22	66.25	68.38	75.78
PSO	67339	47	74.11	63.89	65.42	76.60
OSMO	52092	59	80.19	69.97	73.21	82.25

feature selection methods. The proposed OSMO-based feature selection method selects 52092 features which are 41% of total features. Regarding the feature elimination process, the OSMO eliminates the highest number of features, i.e., 59%, followed by IGSA based algorithm, which reduces the 56% of features. This result reflects that the oscillating

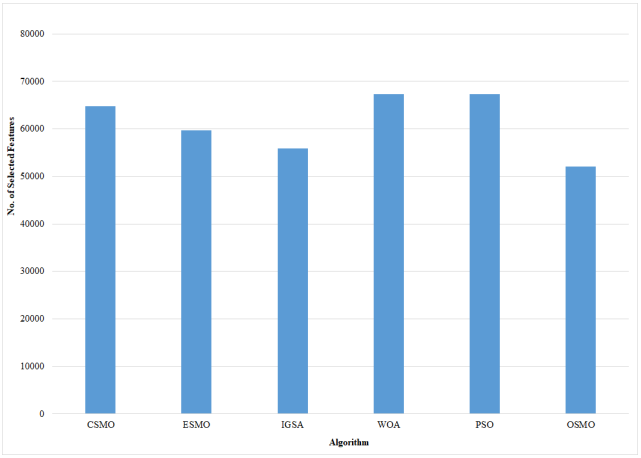

FIGURE 3. Algorithm wise feature selection.

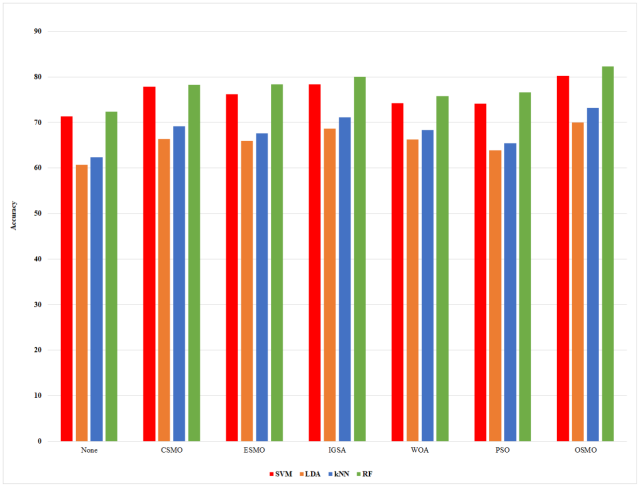

FIGURE 4. Comparison of accuracy for considered algorithms.

perturbation rate helps SMO converge better and gives higher precision values in selecting relevant features than other existing methods.

Four classifiers are used to check the relevancy of the selected features, namely SVM, LDA, kNN, and RF. The returned accuracy from each classifier is depicted in Table 6 and Fig. 4. The RF classifier gives 82.25% accuracy for an OSMO-based approach which is the highest. However, the remaining classifiers also perform better for feature sets selected by OSMO. Therefore, it can be said that the OSMO-based feature selection approach for soil image classification improves other algorithms and can be utilized for other classification applications.

V. CONCLUSION AND FUTURE SCOPE

This work presented a new approach for feature selection from soil images named as oscillating SMO algorithm. An oscillating perturbation is proposed in the OSMO algorithm to take advantage of non-linearity and achieve a better convergence. The OSMO algorithm was tested on 15 benchmarks and compared against CSMO, ESMO, IGSA, WOA, and PSO algorithms. The results show the best convergence behavior of the OSMO algorithm. In addition, the proposed algorithm was tested on a soil image dataset that has seven classes. The proposed OSMO-based feature selection algorithm takes SURF extracted features and eliminates irrelevant and non-redundant features. The work was compared with five other well-known meta-heuristic algorithms, namely CSMO, ESMO, IGSA, WOA, and PSO-based techniques. The proposed OSMO-based algorithm eliminates the maximum number of features, i.e., 59%. Four classifiers are tested to classify soil images: RF, LDA, kNN, and SVM. Table 6 demonstrates that all the classifies give good results for OSMO, but RF gives the best accuracy for it.

The future work includes the applicability of the OSMO to other real-world datasets. Furthermore, the parallelization of OSMO may be implemented for its use in big data. The perturbation rate may be modified with some nonlinear search strategies to take advantage of the nonlinear nature of the problem.

REFERENCES

[1] Z. Wang, H. Li, Y. Zhu, and T. Xu, "Review of plant identification based on image processing," *Arch. Comput. Methods Eng.*, vol. 24, no. 3, pp. 637–654, Jul. 2017.
[2] V. Singh and A. K. Misra, "Detection of plant leaf diseases using image segmentation and soft computing techniques," *Inf. Process. Agricult.*, vol. 4, pp. 41–49, Mar. 2017.
[3] B. Bhattacharya and D. P. Solomatine, "Machine learning in soil classification," *Neural Netw.*, vol. 19, no. 2, pp. 186–195, Mar. 2006.
[4] A. Mishra. *Multi Class Support Vector Machine*. MATLAB Central File Exchange. Accessed: Dec. 15, 2021. [Online]. Available: https://www.mathworks.com/matlabcentral/fileexchange/33170-multi-class-support-vector-machine
[5] B. Bhattacharya and D. P. Solomatine, "An algorithm for clustering and classification of series data with constraint of contiguity," in *Design and Application of Hybrid Intelligent Systems*. Amsterdam, The Netherlands: IOS Press, 2003, pp. 489–498.
[6] P. W. Mayne, *Cone Penetration Testing*, vol. 368. Washington, DC, USA: Transportation Research Board, 2007.
[7] Z. Zhang and M. T. Tumay, "Statistical to fuzzy approach toward CPT soil classification," *J. Geotech. Geoenviron. Eng.*, vol. 125, no. 3, pp. 179–186, Mar. 1999.
[8] K. Srunitha and S. Padmavathi, "Performance of SVM classifier for image based soil classification," in *Proc. Int. Conf. Signal Process., Commun., Power Embedded Syst. (SCOPES)*, Oct. 2016, pp. 411–415.
[9] R. Shenbagavalli and K. Ramar, "Classification of soil textures based on laws features extracted from preprocessing images on sequential and random Windows," *Bonfring Int. J. Adv. Image Process.*, vol. 1, p. 15, Dec. 2011.
[10] S.-O. Chung, K.-H. Cho, J.-W. Kong, K. A. Sudduth, and K.-Y. Jung, "Soil texture classification algorithm using RGB characteristics of soil images," *IFAC Proc. Volumes*, vol. 43, no. 26, pp. 34–38, 2010.
[11] H. K. Sharma and S. Kumar, "Soil classification & characterization using image processing," in *Proc. 2nd Int. Conf. Comput. Methodol. Commun. (ICCMC)*, Feb. 2018, pp. 885–890.
[12] M. Saraswat and K. V. Arya, "Feature selection and classification of leukocytes using random forest," *Med. Biol. Eng. Comput.*, vol. 52, no. 12, pp. 1041–1052, Dec. 2014.
[13] H. Mittal and M. Saraswat, "Classification of histopathological images through bag-of-visual-words and gravitational search algorithm," in *Proc. Int. Conf. Soft Comput. Problem Solving*, 2017, pp. 231–241.
[14] A. A. Cruz-Roa, J. E. A. Ovalle, A. Madabhushi, and F. A. G. Osorio, "A deep learning architecture for image representation, visual interpretability and automated basal-cell carcinoma cancer detection," in *Proc. Int. Conf. Med. Image Comput.-Assist. Intervent.* Berlin, Germany: Springer, 2013, pp. 403–410.

[15] H. Chang, N. Nayak, P. T. Spellman, and B. Parvin, "Characterization of tissue histopathology via predictive sparse decomposition and spatial pyramid matching," in *Proc. Int. Conf. Med. Image Comput.-Assist. Intervent.* Berlin, Germany: Springer, 2013, pp. 91–98.
[16] J. Xu, L. Xiang, Q. Liu, H. Gilmore, J. Wu, J. Tang, and A. Madabhushi, "Stacked sparse autoencoder (SSAE) for nuclei detection on breast cancer histopathology images," *IEEE Trans. Med. Imag.*, vol. 35, no. 1, pp. 119–130, Jul. 2015.
[17] G. Shi, F. Luo, Y. Tang, and Y. Li, "Dimensionality reduction of hyperspectral image based on local constrained manifold structure collaborative preserving embedding," *Remote Sens.*, vol. 13, no. 7, p. 1363, Apr. 2021.
[18] W. Li and Q. Du, "Laplacian regularized collaborative graph for discriminant analysis of hyperspectral imagery," *IEEE Trans. Geosci. Remote Sens.*, vol. 54, no. 12, pp. 7066–7076, Dec. 2016.
[19] J. Padarian, B. Minasny, and A. B. McBratney, "Using deep learning for digital soil mapping," *SOIL*, vol. 5, no. 1, pp. 79–89, Feb. 2019.
[20] Y. Lu, D. Perez, M. Dao, C. Kwan, and J. Li, "Deep learning with synthetic hyperspectral images for improved soil detection in multispectral imagery," in *Proc. 9th IEEE Annu. Ubiquitous Comput., Electron. Mobile Commun. Conf. (UEMCON)*, Nov. 2018, pp. 666–672.
[21] Y. Yu, T. Xu, Z. Shen, Y. Zhang, and X. Wang, "Compressive spectral imaging system for soil classification with three-dimensional convolutional neural network," *Opt. Exp.*, vol. 27, no. 16, pp. 23029–23048, 2019.
[22] N. N. Thuy and S. Wongthanavasu, "A new approach for reduction of attributes based on stripped quotient sets," *Pattern Recognit.*, vol. 97, Jan. 2020, Art. no. 106999.
[23] N. N. Thuy and S. Wongthanavasu, "A novel feature selection method for high-dimensional mixed decision tables," *IEEE Trans. Neural Netw. Learn. Syst.*, early access, Jan. 15, 2021, doi: 10.1109/TNNLS.2020.3048080.
[24] A. Nayyar, D.-N. Le, and N. G. Nguyen, *Advances in Swarm Intelligence for Optimizing Problems in Computer Science*. Boca Raton, FL, USA: CRC Press, 2018.
[25] A. Nayyar and N. G. Nguyen, "Introduction to swarm intelligence," in *Advances in Swarm Intelligence for Optimizing Problems in Computer Science*. Boca Raton, FL, USA: CRC Press, 2018, pp. 53–78.
[26] T. Ojala, M. Pietikäinen, and D. Harwood, "A comparative study of texture measures with classification based on featured distributions," *Pattern Recognit.*, vol. 29, no. 1, pp. 51–59, 1996.
[27] N. Dalal and B. Triggs, "Histograms of oriented gradients for human detection," in *Proc. IEEE Comput. Soc. Conf. Comput. Vis. Pattern Recognit.*, vol. 1, Jun. 2005, pp. 886–893.
[28] H. Bay, A. Ess, T. Tuytelaars, and L. Van Gool, "Speeded-up robust features (SURF)," *Comput. Vis. Image Understand.*, vol. 110, no. 3, pp. 346–359, 2008.
[29] D. G. Lowe, "Distinctive image features from scale-invariant keypoints," *Int. J. Comput. Vis.*, vol. 60, no. 2, pp. 91–110, 2004.
[30] S. Bhattacharyya, A. Sengupta, T. Chakraborti, A. Konar, and D. N. Tibarewala, "Automatic feature selection of motor imagery EEG signals using differential evolution and learning automata," *Med. Biol. Eng. Comput.*, vol. 52, no. 2, pp. 131–139, Feb. 2014.
[31] H. Deng and G. Runger, "Feature selection via regularized trees," in *Proc. Int. Joint Conf. Neural Netw. (IJCNN)*, Jun. 2012, pp. 1–8.
[32] M. A. Hall, "Correlation-based feature selection of discrete and numeric class machine learning," Dept. Comput. Sci., Univ. Waikato, Hamilton, New Zealand, Work. Paper 00/08, 2000.
[33] S. F. Cotter, K. Kreutz-Delgado, and B. D. Rao, "Backward sequential elimination for sparse vector subset selection," *Signal Process.*, vol. 81, no. 9, pp. 1849–1864, Sep. 2001.
[34] I. Guyon, J. Weston, S. Barnhill, and V. Vapnik, "Gene selection for cancer classification using support vector machines," *Mach. Learn.*, vol. 46, nos. 1–3, pp. 389–422, 2002.
[35] G. Roffo, S. Melzi, U. Castellani, A. Vinciarelli, and M. Cristani, "Infinite feature selection: A graph-based feature filtering approach," *IEEE Trans. Pattern Anal. Mach. Intell.*, vol. 43, no. 12, pp. 4396–4410, Dec. 2021.
[36] A. Hashemi, M. B. Dowlatshahi, and H. Nezamabadi-pour, "MGFS: A multi-label graph-based feature selection algorithm via pagerank centrality," *Expert Syst. Appl.*, vol. 142, Mar. 2020, Art. no. 113024.
[37] K. Henni, N. Mezghani, and C. Gouin-Vallerand, "Unsupervised graph-based feature selection via subspace and pagerank centrality," *Expert Syst. Appl.*, vol. 114, pp. 46–53, Dec. 2018.
[38] G. Roffo, S. Melzi, U. Castellani, and A. Vinciarelli, "Infinite latent feature selection: A probabilistic latent graph-based ranking approach," in *Proc. IEEE Int. Conf. Comput. Vis. (ICCV)*, Oct. 2017, pp. 1398–1406.
[39] Z. Zhang and E. R. Hancock, "A graph-based approach to feature selection," in *Proc. Int. Workshop Graph-Based Represent. Pattern Recognit.* Berlin, Germany: Springer, 2011, pp. 205–214.
[40] X. Chen, T. Fang, H. Huo, and D. Li, "Graph-based feature selection for object-oriented classification in VHR airborne imagery," *IEEE Trans. Geosci. Remote Sens.*, vol. 49, no. 1, pp. 353–365, Jan. 2011.
[41] J. C. Bansal, H. Sharma, S. S. Jadon, and M. Clerc, "Spider monkey optimization algorithm for numerical optimization," *Memetic Comput.*, vol. 6, no. 1, pp. 31–47, Mar. 2014.
[42] A. Chugh, V. K. Sharma, S. Kumar, A. Nayyar, B. Qureshi, M. K. Bhatia, and C. Jain, "Spider monkey crow optimization algorithm with deep learning for sentiment classification and information retrieval," *IEEE Access*, vol. 9, pp. 24249–24262, 2021.
[43] S. Kumar, B. Sharma, V. K. Sharma, and R. C. Poonia, "Automated soil prediction using bag-of-features and chaotic spider monkey optimization algorithm," *Evol. Intell.*, vol. 14, pp. 293–304, Jun. 2018.
[44] S. Kumar, B. Sharma, V. K. Sharma, H. Sharma, and J. C. Bansal, "Plant leaf disease identification using exponential spider monkey optimization," *Sustain. Comput., Informat. Syst.*, vol. 28, Dec. 2020, Art. no. 100283.
[45] X.-S. Yang, *Nature-Inspired Optimization Algorithms*. Amsterdam, The Netherlands: Elsevier, 2014.
[46] D. Simon, *Evolutionary Optimization Algorithms*. Hoboken, NJ, USA: Wiley, 2013.
[47] M. Jamil and X.-S. Yang, "A literature survey of benchmark functions for global optimisation problems," *Int. J. Math. Model. Numer. Optim.*, vol. 4, no. 2, pp. 150–194, 2013.
[48] J. C. Bansal, P. Singh, M. Saraswat, A. Verma, S. S. Jadon, and A. Abraham, "Inertia weight strategies in particle swarm optimization," in *Proc. 3rd World Congr. Nature Biol. Inspired Comput.*, 2011, pp. 633–640.
[49] S. Mirjalili and A. Lewis, "The whale optimization algorithm," *Adv. Eng. Softw.*, vol. 95, pp. 51–67, May 2016.
[50] H. Askari and S.-H. Zahiri, "Decision function estimation using intelligent gravitational search algorithm," *Int. J. Mach. Learn. Cybern.*, vol. 3, no. 2, pp. 163–172, Jun. 2012.
[51] J. Kennedy and R. Eberhart, "Particle swarm optimization," in *Proc. IEEE Int. Conf. Neural Netw.* Princeton, NJ, USA: Citeseer, vol. 4, Nov./Dec. 1995, pp. 1942–1948.
[52] J. Derrac, S. García, D. Molina, and F. Herrera, "A practical tutorial on the use of nonparametric statistical tests as a methodology for comparing evolutionary and swarm intelligence algorithms," *Swarm Evol. Comput.*, vol. 1, no. 1, pp. 3–18, Mar. 2011.

RAHUL AGARWAL received the B.E. degree in information technology from DSCE, Bengaluru, in 2004, and the M.Tech. degree from the Department of Computer Engineering, Central University, Ajmer, in 2012. He has been working as an Assistant Professor with the Government Engineering College Bikaner, since 2007. He has published two research papers in reputed journals and conferences.

NARPAT SINGH SHEKHAWAT received the M.S. degree in computer engineering from BITS Pilani, in 2009, and the Ph.D. degree from the Department of Computer Engineering, SGVU University, Jaipur, in 2013. He has been working as an Assistant Professor with the Government Engineering College Bikaner, since 2001. He has published six research papers in reputed journals and conferences. He is a member of CSI and ISTE.

SANDEEP KUMAR (Member, IEEE) received the Bachelor of Engineering degree from the Engineering College Kota, in 2005, the Master of Technology degree from RTU Kota, in 2011, and the Ph.D. degree in computer science & engineering from Jagannath University, Jaipur, in 2015. He is currently an Associate Professor at CHRIST (Deemed to be University), Bengaluru, India, and a Postdoctoral Research Fellow with Imam Muhammad Ibn Saud Islamic University, Riyadh, Saudi Arabia. He has worked with ACEIT Jaipur, Jagannath University, Jaipur, and Amity University Rajasthan. He is currently an Associate Editor of the *Human-centric Computing and Information Sciences* (HCIS) journal, (Springer). He has published more than 70 research articles in well-known SCI/SCOPUS indexed international journals and conferences and attended several national and international conferences and workshops. He has authored/edited five books in the area of computer science. His research interests include nature-inspired algorithms, swarm intelligence, soft computing, and computational intelligence.

ANAND NAYYAR (Senior Member, IEEE) received the Ph.D. degree in computer science from Desh Bhagat University, in the area of wireless sensor networks and swarm intelligence, in 2017. He is currently working with the School of Computer Science-Duy Tan University, Da Nang, Vietnam, as an Assistant Professor, the Scientist, the Vice-Chairperson (Research), and the Director of the IoT and Intelligent Systems Laboratory. A Certified Professional with more than 75 professional certificates from CISCO, Microsoft, Oracle, Google, Beingcert, EXIN, GAQM, and Cyberoam. He has published more than 125 research papers in various High-Quality ISI-SCI/SCIE/SSCI Impact Factor Journals cum Scopus Journals, more than 50 papers in international conferences indexed with Springer, IEEE Xplore and ACM Digital Library, more than 40 book chapters in various Scopus, Web of Science Indexed Books with Springer, CRC Press, Elsevier, and many more with Citations of more than 4500, H-Index of 36, and I-Index of 122. He is a member of more than 50 associations as a Senior and Life Member. He has authored/co-authored cum edited more than 30 books of computer science. He has associated with more than 500 international conferences as a Programme Committee/the Chair/an Advisory Board/a Review Board Member. He has 11 Australian patents, five Indian patents, one Indian copyright to his credit in the area of wireless communications, artificial intelligence, cloud computing, the IoT, and image processing. He was awarded more than 32 awards for teaching and research, such as Young Scientist, Best Scientist, Young Researcher Award, Outstanding Researcher Award, Excellence in Teaching and many more. He is acting as an Associate Editor of *Wireless Networks*, (Springer), *Computer Communications*, (Elsevier), *International Journal of Sensor Networks* (IJSNET), (Inderscience), *Frontiers in Computer Science*, *PeerJ Computer Science*, *Human-centric Computing and Information Sciences* (HCIS), *IET-Quantum Communications*, *IET Wireless Sensor Systems*, *IET Networks*, *IJDST*, *IJISP*, *IJCINI*, and *IJGC*. He is acting as the Editor-in-Chief of IGI-Global, USA Journal titled *International Journal of Smart Vehicles and Smart Transportation* (IJSVST). He has reviewed more than 1400 articles for various web of science indexed journals. He is currently researching in the area of wireless sensor networks, the IoT, swarm intelligence, cloud computing, artificial intelligence, drones, blockchain, cyber security, network simulation and wireless communications.

BASIT QURESHI (Member, IEEE) received the bachelor's degree in computer science from Ohio University, Athens, OH, USA, in 2000, the master's degree in computer science from Florida Atlantic University, in 2002, and the Ph.D. degree in computer science from the University of Bradford, U.K., in 2011. He is currently an Associate Professor and the Chair of the Department of Computer Science, Prince Sultan University, Saudi Arabia. He has published over 60 research works in the area of robotics, the Internet of Things, machine learning, and computational intelligence. He is a member of the IEEE Computer Society, the IEEE Communications Society, and the ACM.